General Disclaimer

One or more of the Following Statements may affect this Document

- This document has been reproduced from the best copy furnished by the organizational source. It is being released in the interest of making available as much information as possible.

- This document may contain data, which exceeds the sheet parameters. It was furnished in this condition by the organizational source and is the best copy available.

- This document may contain tone-on-tone or color graphs, charts and/or pictures, which have been reproduced in black and white.

- This document is paginated as submitted by the original source.

- Portions of this document are not fully legible due to the historical nature of some of the material. However, it is the best reproduction available from the original submission.

Produced by the NASA Center for Aerospace Information (CASI)

AD616343

MIE SCATTERING AND ABSORPTION CROSS SECTIONS FOR ABSORBING PARTICLES

by

Gilbert N. Plass
Southwest Center for Advanced Studies
Dallas, Texas

Submitted to Applied Optics
May, 1965

COPY ___ OF ___
HARD COPY $. 2.00
MICROFICHE $. 0.50
32p

This work was supported by the Air Force Cambridge Research Laboratories, Office of Aerospace Research contract AF19(628)-5039 and by the National Aeronautics and Space Administration contract NsG-269-62.

DDC
JUN 18 196
TISIA E

EVALUATION COPY

PROCESSING COPY

ARCHIVE COPY

MIE SCATTERING AND ABSORPTION CROSS SECTIONS FOR ABSORBING PARTICLES

Gilbert N. Plass

Abstract

The Mie scattering and absorption cross sections for spherical particles are calculated as a function of the complex index of refraction, $n = n_1 - in_2$. Curves of the efficiency factors for absorption, scattering, and extinction are given for n_1 = 1.01, 1.33, 1.5, 2 and for $n_2 = 10^{-4}$, 10^{-2}, 10^{-1}, 1, and 10. The influence of the absorption on the efficiency factors is discussed. The results are compared with previously proposed simplified expressions for these factors. The variation of the scattered intensity with angle as n_2 is varied is illustrated in some typical cases. Finally the influence of n_2 on the narrow resonances which occur for large values of n_1 is discussed.

The author is with the Southwest Center for Advanced Studies, P. O. Box 30365, Dallas, Texas 75230.

Received

This work was supported by the Air Force Cambridge Research Laboratories, Office of Aerospace Research and by the National Aeronautics and Space Administration.

I. Introduction

The interaction of electromagnetic radiation with absorbing spheres is a problem which arises in many different branches of science. Absorbing particles occur abundantly in planetary atmospheres where their interaction with ultraviolet, visible, and infrared radition is of great importance. Astrophysicists are interested in the modification of light by interstellar particles. Numerous applications occur in chemistry when the size distribution and composition of mixtures containing small particles is studied. Van de Hulst's book[1] is now the classic reference which discusses the Mie theory in detail together with many of its applications.

Until the advent of modern high-speed computors, relatively few Mie theory calculations had been done for absorbing particles. Simplified equations were developed for a few limiting cases. The few calculations which were performed are reviewed by Van de Hulst[1]. Extensive computations for particular absorbing substances have been performed with the aid of high speed computors. These calculations have been made for carbon[2], aluminum and magnesium oxide[3,4], and particularly water droplets (the literature on this subject is reviewed by Deirmendjian et al.[5,6]).

It is difficult to obtain an understanding of the behavior of the cross sections for absorbing particles from these results which were calculated for the particular values of the complex index of refraction appropriate for these particular substances.

Aside from the general discussion in Van de Hulst's book[1] the only attempt at understanding the general behavior of these cross sections has been made by Deirmendjian et al.[5] Although these authors discuss very clearly many of the general characteristics of these cross sections, their illustrations are again given for only a few particular values of the index.

In the present study the Mie cross sections are calculated for a wide range of complex indices of refraction. The particular values chosen do not necessarily correspond to real substances, but rather are intended to illustrate the variation in the cross sections as the absorption by the particle varies over a wide range. These results are then compared with some of the limiting approximations which have been proposed.

II. Absorption Cross Section

The complex index of refraction is the sole physical parameter which determines the absorption and scattering of an electromagnetic wave by a spherical particle with a given ratio of radius to wavelength. The Mie theory[7] has been extensively described in the literature[1]. Some time ago an efficient program for the calculation of Mie scattering and absorption cross sections was developed by Stull and Plass[2] for use on an electronic computor. The details of the method are given in that paper. More recently some valuable improvements in the original program were made by P. J. Wyatt.

The results of the exact calculations for the absorption cross section made by this method are given by the solid curves of Figs. 1-4 with n_1 = 1.01; 1.33; 1.5; 2.0 (where the index of refraction is written $n = n_1 - in_2$) and for a range of n_2 from zero to 10. The efficiency factor for absorption, Q_{abs}, (absorption cross section divided by corss-sectional area of particle) is plotted as a function of $x = 2\pi a/\lambda$, where a is the radius of the particle and λ is the wavelength.

One of the first features which one observed from these curves (and from further calculations which could not be shown here) is that Q_{abs} = (constant)n_2 for a fixed value of x and n_1, provided only that $n_2 \leq 0.01$. Thus, if a curve of Q_{abs} as a function of x is calculated for a particular n_1 and for one value of $n_2 < 0.01$, then Q_{abs} is known immediately for all other values of n_2 which satisfy the inequality. A linear dependence of Q_{abs} on n_2 is to be expected, of course, when the absorption by the particle is sufficiently small.

The curves for Q_{abs} vary smoothly with x for n_1 = 1.01 and 1.33, but for larger values of n_1 some resonances appear. The qualitative appearance of the curves is the same in each of these figures, except for these minor resonances. For $n_2 \leq 0.1$ the curves gradually approach their limiting values for large x from below. The curves for n_2 = 1 and 10 reach a maximum value (the maximum value of Q_{abs} in all cases reported here is near 1.8 for n_2 = 1) and approach their limiting values for large x from above. In almost all cases Q_{abs} increases slightly as n_1 increases while n_2 and x are held fixed.

An approximate equation for Q_{abs} was proposed by Van de Hulst[1],

$$Q_{abs} = 2K(4xn_2) \quad , \tag{1}$$

where the function K is

$$K(w) = (1/2) + w^{-1}e^{-w} + w^{-2}(e^{-w}-1) \quad . \tag{2}$$

This equation is expected to be useful when both $n_1 - 1 \ll 1$ and $n_2 \ll 1$.

For comparison purposes Eq. (1) is plotted as a dashed curve in Figs. 1-3. For $n_1 = 1.01$, the two curves coincide for $n_2 \leq 10^{-2}$ on the scale of Fig. 1. There are relatively small differences between the curves for $n_2 = 10^{-1}$. For $n_2 = 1$, the approximate curve fails to reproduce the maximum and becomes more and more inexact as x becomes larger. The approximate equation fails entirely for $n_2 = 10$. When $n_1 = 1.33$ or 1.5, the descrepencies between the two curves are fairly large even for small values of n_2, as is shown in Figs. 2 and 3. It should be noted that Eq. (1) is independent of n_1 and thus does not reproduce the slow increase of Q_{abs} with n_1 for a fixed x and n_2. For this reason Eq. (1) is not plotted in Fig. 4, as it is no longer a reasonable approximation to the exact curve.

For most values of x, the maximum value of Q_{abs} occurs for n_2 in the range from 0.1 to 1. The value of Q_{abs} is an order of magnitude less when n_2 increases to 10. The reason

for this behavior is that, when $n_2 = 10$, over 90% of the incident radiation is reflected, whereas only about 20% is reflected when $n_2 = 1$ for the values of n_1 considered here.

III. Scattering Cross Sections

The efficiency factors for scattering are shown in Figs. 5-8 for $n_1 = 1.01, 1.33, 1.5, 2.0$. For small values of Q_{sca} before the first maximum in the curve, Q_{sca} increases approximately as x^2, whereas Q_{abs} increases as x.

The values of Q_{sca} are the same on the scale of these figures for all $n_2 \leq 10^{-4}$ (actually the values do not vary by more than 2 units in the third significant figure over this entire range).

The influence of n_2 on Q_{sca} is rather complicated. In Fig. 5 it is seen that, when $x < 30$ and $n_1 = 1.01$, Q_{sca} increases as n_2 increases from zero to 10. Because of the small value of n_1, the first resonance lies beyond $x = 30$ for small n_2. However, for $n_2 = 1$ and 10, the maximum of the curve occurs at x values of about 3 and 1.3 respectively.

The curves in Figs. 6-8 show a number of resonances. The value of Q_{sca} always <u>decreases</u> at first as n_2 increases whenever x is greater than about 2. When $n_2 = 10^{-2}$, the second maximum of the curve is appreciably lower than when $n_2 \leq 10^{-4}$. The succeeding waves in the curve are slowly damped out for $n_2 = 10^{-2}$. When $n_2 = 0.1$, only a few maxima can be seen in the curve before the waves are completely damped out. When $n_2 = 1$ or 10 the curve has only one maximum and then decreases very slowly to its limiting value. Parts of these curves are above the

curves for smaller n_2 values. For the range of n_1 shown here the limiting value of Q_{sca} as x becomes very large is between 1.00 and 1.11 when $n_2 \leq 0.1$, is about 1.2 when $n_2 = 1$, and is near 1.95 when $n_2 = 10$.

IV. Extinctions Cross Section

The extinction efficiency factors for $n_1 = 1.01$, 1.33, 1.5, 2.0 are shown in Figs. 9-12. Although this factor is merely the sum of the absorption and scattering efficiency factors, it seems worthwhile to present these curves because (1) curves on a linear rather logarithmic scale present different information; (2) the absorption and scattering efficiency factors make varying contributions to the whole as the parameters change; (3) a comparison with Van der Hulst's simplified equation is instructive.

The approximate equation for Q_{ext} proposed by Van der Hulst[1] is

$$Q_{ext} = 2-4 \exp(-\rho \tan\beta)(\rho^{-1}\cos\beta)\sin(\rho-\beta) \qquad (3)$$

$$-4\exp(-\rho\tan\beta)(\rho^{-1}\cos\beta)^2\cos(\rho-2\beta) + 4(\rho^{-1}\cos\beta)^2\cos 2\beta,$$

where

$$\rho = 2x(n_1-1) \quad , \qquad (4)$$

$$\tan\beta = n_2(n_1-1)^{-1} \qquad (5)$$

This equation is valid under the same conditions as Eq. (1). Equation (3) is plotted as a dashed line in Figs. 9-11.

Again the approximate and true curves are indistinguishable when $n_1 = 1.01$ and $n_2 \leq 10^{-2}$. There are slight differences when $n_2 = 10^{-1}$. As expected Eq. (3) breaks down when $n_2 \geq 1$ and does not reproduce the true curve.

When $n_1 = 1.33$ and 1.5, Eq. (3) reproduces the qualitative shape of the curves for $n_2 \leq 10^{-1}$. Nevertheless the actual values of the maxima and minima are poorly reproduced. Deirmendjian[8] has proposed an empirical formula which corrects this deficiency in Eq. (3). However, we have not compared it in detail with our results because of its complexity and because it does not appear to increase appreciably the range of validity of Eq. (3).

The curves for very small values of n_2 do not attempt to represent the many small ripples which exist in these curves[1]. These are rapidly damped out as n_2 increases. As x increases, Q_{ext} always approaches the value 2. As n_1 increases, the first resonance in the curve becomes larger and narrower and occurs at smaller x values. It is virtually completely damped out when $n_2 = 1$.

The curve for $n_2 = 10^{-1}$ in Fig. 12 illustrates how the resonances can be damped out as x increases. For $x < 15$ this curve has maxima and minima at the same positions as the curve for smaller n_2 values. However, as x becomes greater than 15 an elementary calculation shows that there is no longer any appreciable transmitted energy through the particle; all of the radiation which is not reflected is absorbed by the particle.

Thus this curve stops oscillating and decreases slowly in value as x increases further. The same effect can be seen in Figs. 10 and 11.

V. Angular Scattering

It is obviously impossible to show more than a few of the angular scattering patterns which were generated in this study. An illustrative sampling of some typical patterns is shown in Figs. 13-15. These figures are all drawn for the value $x = 5$ and for the values $n_1 = 1.33$, 1.5 and 2 and n_2 from 0 to 10. The solid curves are for the intensity i_1 and the dashed curves for i_2 (as defined by Van de Hulst[1]). The values were calculated every 5° and occasionally more closely when the curve varied rapidly.

The scattering diagrams for each of these values of n_1 exhibit the same pattern of change as n_2 increases. There are only minor variations in the shape of the curves as long as $n_2 \leq 10^{-2}$. When $n_2 = 0.1$, the minima in the curve for i_1 either become more prominent and often sharper ($n_1 = 1.33$ and 1.5) or tend to disappear and become broader ($n_1 = 1.5$ and 2). On the other hand i_2 seems always to develop deeper minima which become more pronounced as n_2 increases to the value 10. The minima of i_1 nearly disappear as n_2 increases to the value 10. The scattering diagrams are most sensitive to the value of n_1 when n_2 is small and are nearly independent of n_1 when $n_2 = 10$.

The values of the intensity at 0° and 180° are marked on the curve. It is interesting to note that the ratio of backward to forward scattering always decreases at first as n_2 increases. The ratio is a minimum when n_2 is between 10^{-2} and 1 and then increases again for larger values of n_2.

VI. Resonances

As n_1 becomes larger more and more resonances occur below a particular, but sufficiently large value of x. The effect on these resonances of absorption by the particle is illustrated in Fig. 16. When $n_1 = 50$ the first resonance due to the magnetic dipole term occurs at $x = 0.0627$. Both the efficiency factors for scattering and absorption have a sharp maximum at this value (unless $n_2 >> 1$).

The values of Q_{abs} are proportional to n_2 when $n_2 \leq 10^{-2}$. The same relationship holds for $n_2 = 0.1$ and 1 provided in addition that $Q_{abs} < 0.1$. The maximum value of Q_{abs} at the resonance peak occurs when $n_2 = 0.1$ and decreases for larger values of n_2. The half-width of the resonance is constant for any $n_2 \leq 0.1$, but increases as n_2 becomes larger than 0.1. The resonance is relatively very broad for $n_2 = 10$ with the half-width several orders of magnitude larger than for values of $n_2 \leq 0.1$.

The resonance in Q_{sca} occurs even if there is no absorption by the particle. The curves for different n_2 values are identical on the scale of Fig. 16 as long as $n_2 \leq 10^{-2}$. The resonance

is so narrow that the maximum value can not be computed accurately. The value of Q_{sca} anywhere near the resonance decreases uniformly as n_2 increases. The resonance has broadened appreciably when $n_2 = 1$ and can no longer be seen in the curve for $n_2 = 10$.

REFERENCES

1. H. C. Van de Hulst, Light Scattering by Small Particles (Wiley, New York, 1957).
2. V. R. Stull and G. N. Plass, J. Opt. Soc. Am. 50, 121 (1960).
3. G. N. Plass, Appl. Opt. 3, 867 (1964).
4. G. N. Plass, Appl. Opt. (submitted for publication).
5. D. Deirmendjian, R. Clasen, and W. Viezee, J. Opt. Soc. Am. 51, 620 (1961).
6. D. Deirmendjian, Appl. Opt. 3, 187 (1964).
7. G. Mie, Ann. Physik 25, 377 (1908).
8. D. Deirmendjian, Quart. J. Roy. Meteorological Soc., 86, 371 (1960).

LEGENDS FOR FIGURES

Fig. 1 Efficiency factor for absorption as a function of $x = 2\pi a/\lambda$, where a is the particle radius and λ is the wavelength for $n_1 = 1.01$. Curves are shown for $n_2 = 10^{-4}$, 10^{-2}, 10^{-1}, 1, 10. The solid curves are the exact results and the dashed curves are the approximate Eq. (1). These curves coincide on this scale for $n_2 = 10^{-4}$ and 10^{-2}.

Fig. 2 Efficiency factor for absorption as a function of $x = 2\pi a/\lambda$ for $n_1 = 1.33$. The solid curves are the exact results and the dashed curves are the approximate Eq. (1).

Fig. 3 Efficiency factor for absorption as a function of $x = 2\pi a/\lambda$ for $n_1 = 1.5$. The solid curves are the exact results and the dashed curves are the approximate Eq. (1).

Fig. 4 Efficiency factor for absorption as a function of $x = 2\pi a/\lambda$ for $n_1 = 2$.

Fig. 5 Efficiency factor for scattering as a function of $x = 2\pi a/\lambda$ for $n_1 = 1.01$.

Fig. 6 Efficiency factor for scattering as a function of $x = 2\pi a/\lambda$ for $n_1 = 1.33$.

Fig. 7 Efficiency factor for scattering as a function of $x = 2\pi a/\lambda$ for $n_1 = 1.5$.

Fig. 8 Efficiency factor for scattering as a function of $x = 2\pi a/\lambda$ for $n_1 = 2$.

Fig. 9 Efficiency factor for extinction as a function of $x = 2\pi a/\lambda$ for $n_1 = 1.01$. The solid curves are the exact results and the dashed curves are the approximate Eq. (3). These curves coincide on this scale for $n_2 = 10^{-4}$ and 10^{-2}.

Fig. 10 Efficiency factor for extinction as a function of $x = 2\pi a/\lambda$ for $n_1 = 1.33$. The solid curves (use left-hand scale) are the exact results and the dashed curves (use right-hand scale) are the approximate Eq. (3).

Fig. 11 Efficiency factor for extinction as a function of $x = 2\pi a/\lambda$ for $n_1 = 1.5$. The solid curves (use left-hand scale) are the exact results and the dashed curves (use right-hand scale) are the approximate Eq. (3).

Fig. 12 Efficiency factor for extinction as a function of $x = 2\pi a/\lambda$ for $n_1 = 2$.

Fig. 13 Scattered intensity as a function of scattering angle for $n_1 = 1.33$ and $x = 2\pi a/\lambda = 5$. The solid curve is the intensity i_1 (as defined by Van de Hulst[1]) and the dashed curve is the intensity i_2. The logarithm of the intensity (1 division = a factor 10) is plotted against the scattering angle. The values of the intensity at 0° and 180° are indicated above the curves near the margin.

Fig. 14 Scattered intensity as a function of scattering angle for $n_1 = 1.5$ and $x = 2\pi a/\lambda = 5$. See caption for Fig. 13.

Fig. 15 Scattered intensity as a function of scattering angle for $n_1 = 2$ and $x = 2\pi a/\lambda = 5$. See caption for Fig. 13.

Fig. 16 Efficiency factors for both absorption and scattering as a function of $x = 2\pi a/\lambda$ for $n_1 = 50$ and various values of n_2. The curves for scattering coincide on this scale for $n_2 \leq 10^{-2}$.

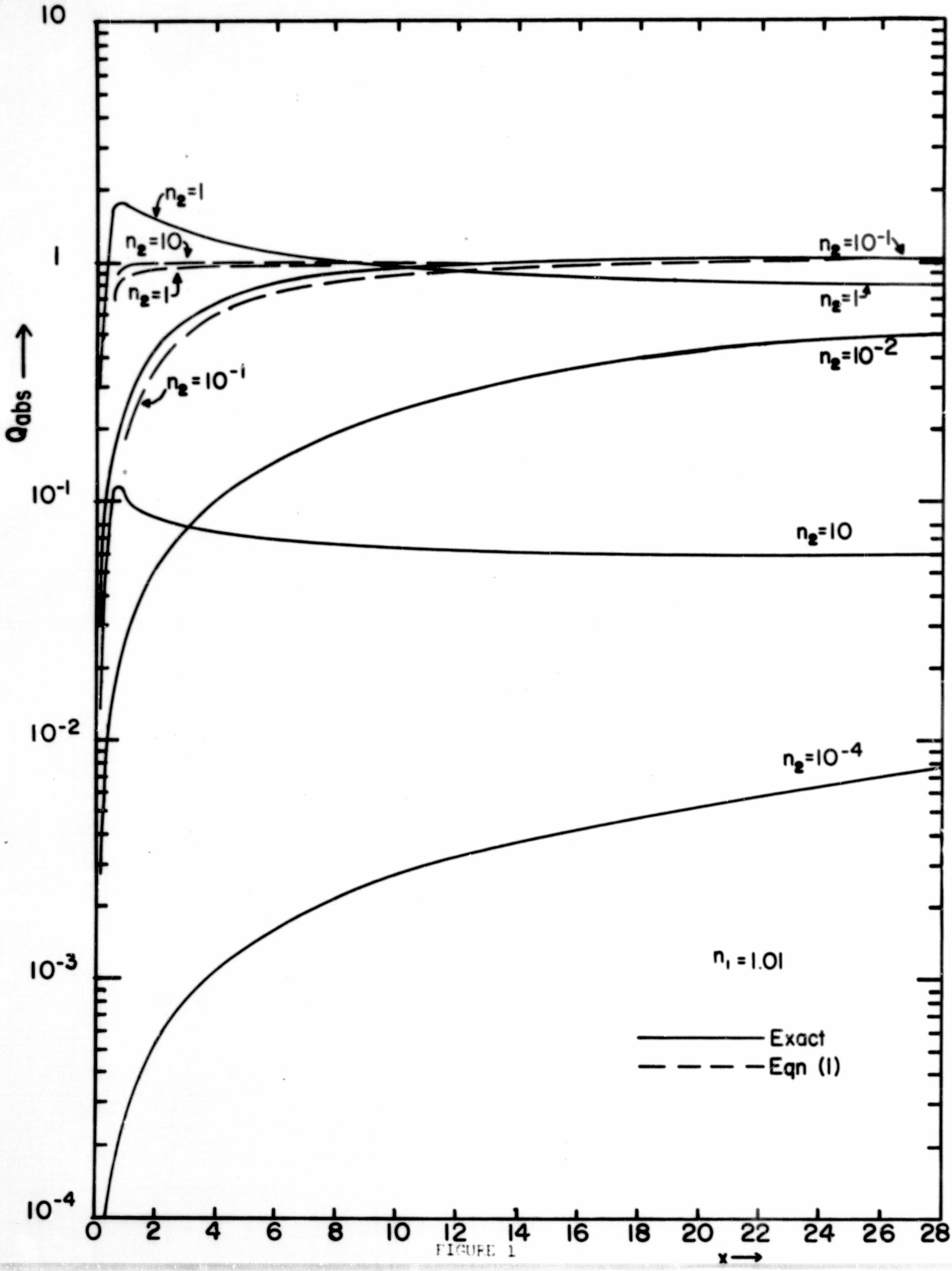
10
1
10^{-1}
10^{-2}
10^{-3}
10^{-4}
Q_{abs} ⟶
$n_2=1$
$n_2=10$
$n_2=1$
$n_2=10^{-1}$
$n_2=10^{-1}$
$n_2=1$
$n_2=10^{-2}$
$n_2=10$
$n_2=10^{-4}$
$n_1=1.01$
Exact
Eqn (1)
0 2 4 6 8 10 12 14 16 18 20 22 24 26 28
x ⟶

FIGURE 1

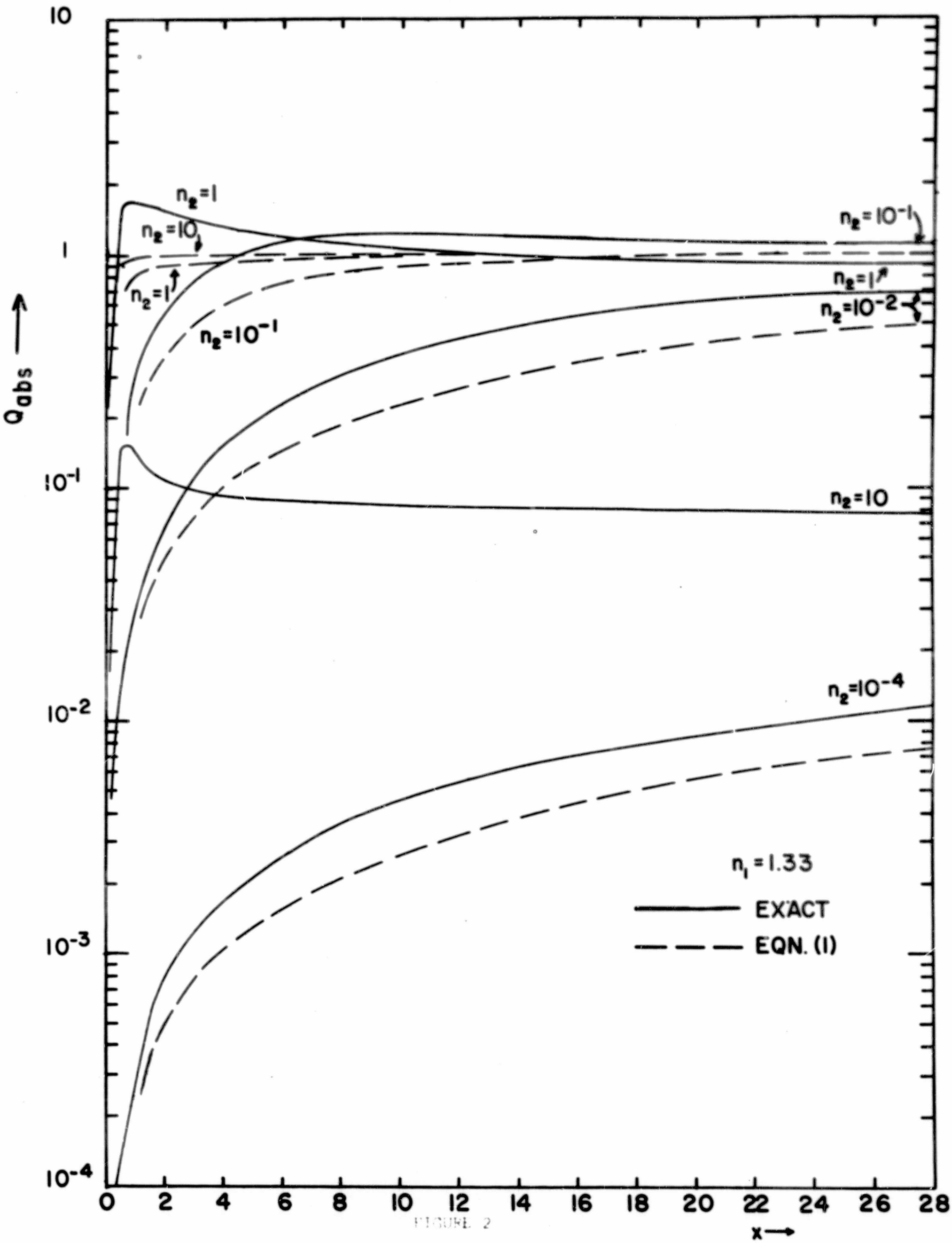
10
1
10^{-1}
10^{-2}
10^{-3}
10^{-4}
Q_{abs} ⟶
$n_2=1$
$n_2=10$
$n_2=1$
$n_2=10^{-1}$
$n_2=10^{-1}$
$n_2=1$
$n_2=10^{-2}$
$n_2=10$
$n_2=10^{-4}$
$n_1=1.33$
EXACT
EQN. (1)
0 2 4 6 8 10 12 14 16 18 20 22 24 26 28
x⟶

FIGURE 2

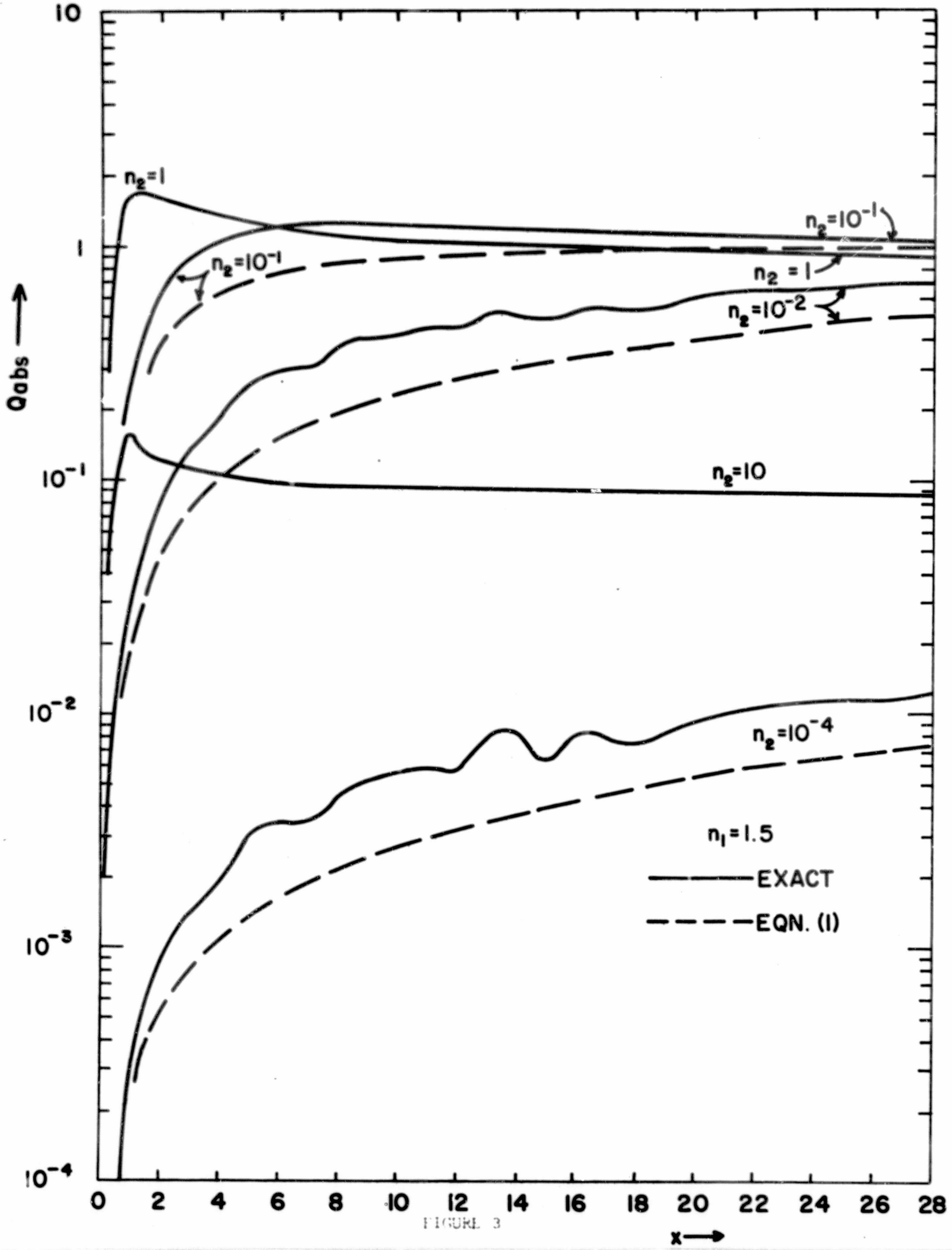
10
1
10^{-1}
10^{-2}
10^{-3}
10^{-4}
Qabs
n_2=1
n_2=10^{-1}
n_2=10^{-1}
n_2 = 1
n_2=10^{-2}
n_2=10
n_2=10^{-4}
n_1=1.5
EXACT
EQN. (1)
0
2
4
6
8
10
12
14
16
18
20
22
24
26
28
x

FIGURE 3

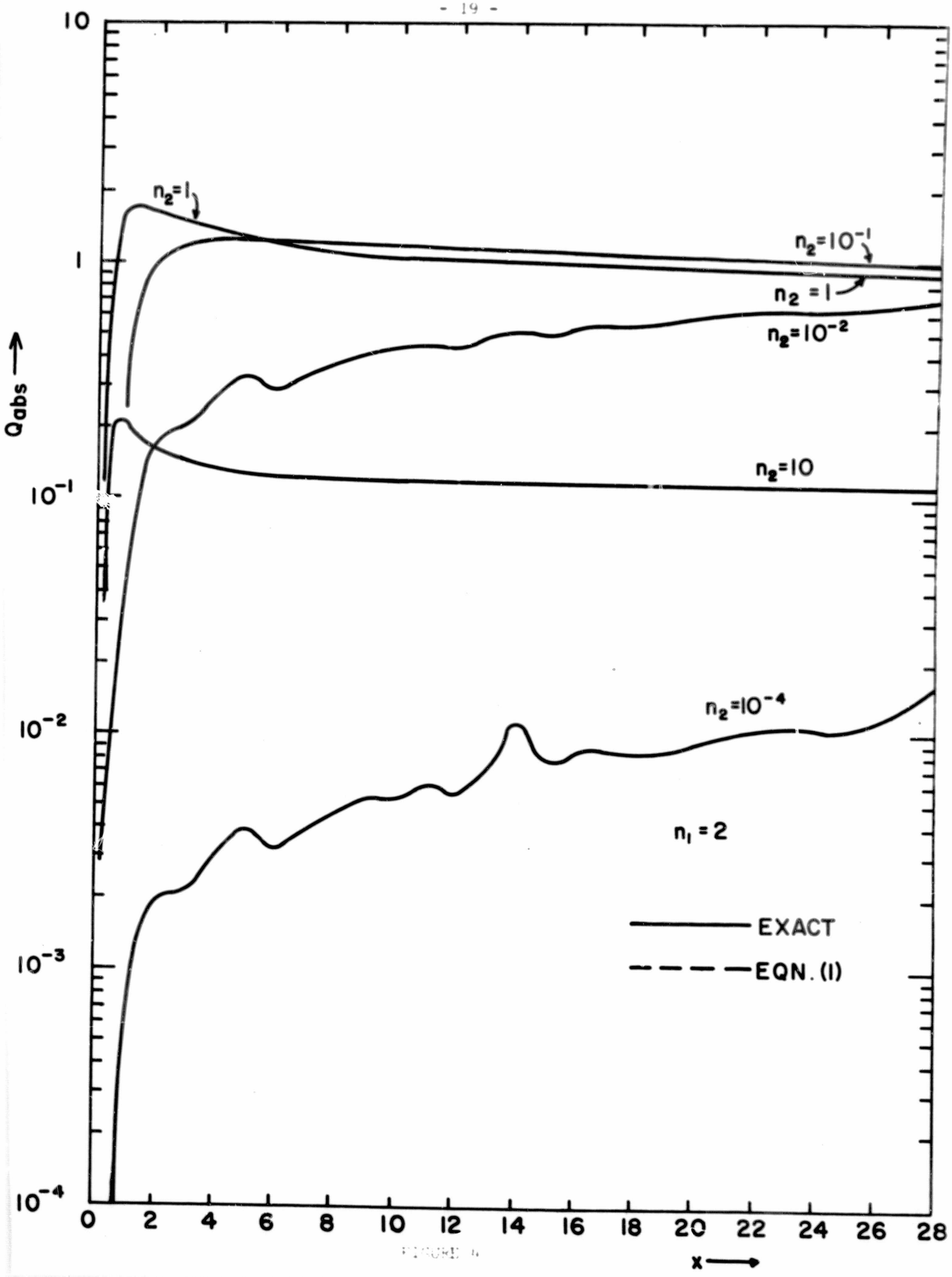
10
1
10^{-1}
10^{-2}
10^{-3}
10^{-4}
Q_{abs} ⟶
$n_2=1$
$n_2=10^{-1}$
$n_2=1$
$n_2=10^{-2}$
$n_2=10$
$n_2=10^{-4}$
$n_1=2$
EXACT
EQN. (1)
0
2
4
6
8
10
12
14
16
18
20
22
24
26
28
x ⟶

FIGURE 4

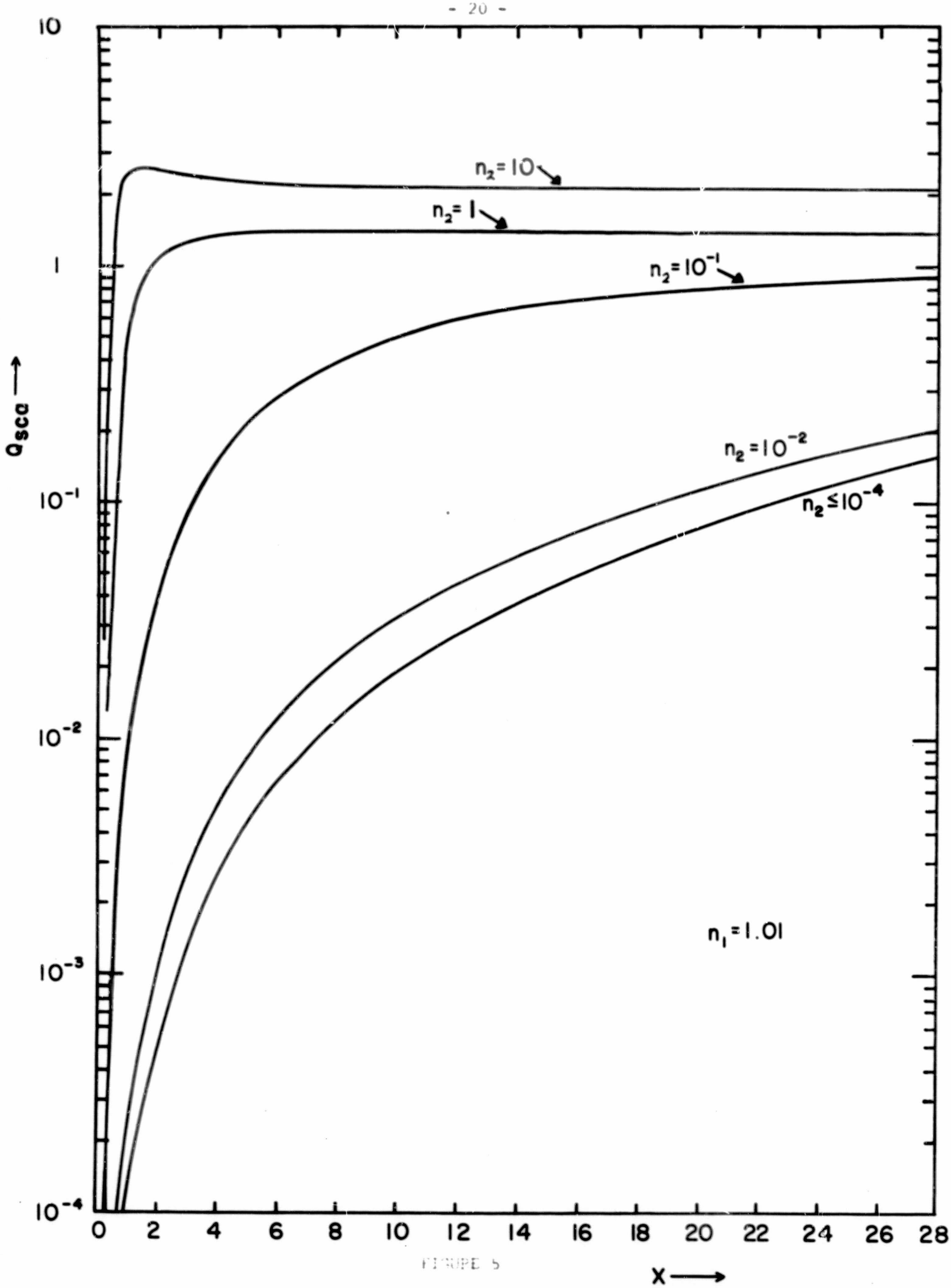
10
1
10^{-1}
10^{-2}
10^{-3}
10^{-4}
Q_{sca} ⟶
$n_2 = 10$
$n_2 = 1$
$n_2 = 10^{-1}$
$n_2 = 10^{-2}$
$n_2 \leq 10^{-4}$
$n_1 = 1.01$
0 2 4 6 8 10 12 14 16 18 20 22 24 26 28
X ⟶

FIGURE 5

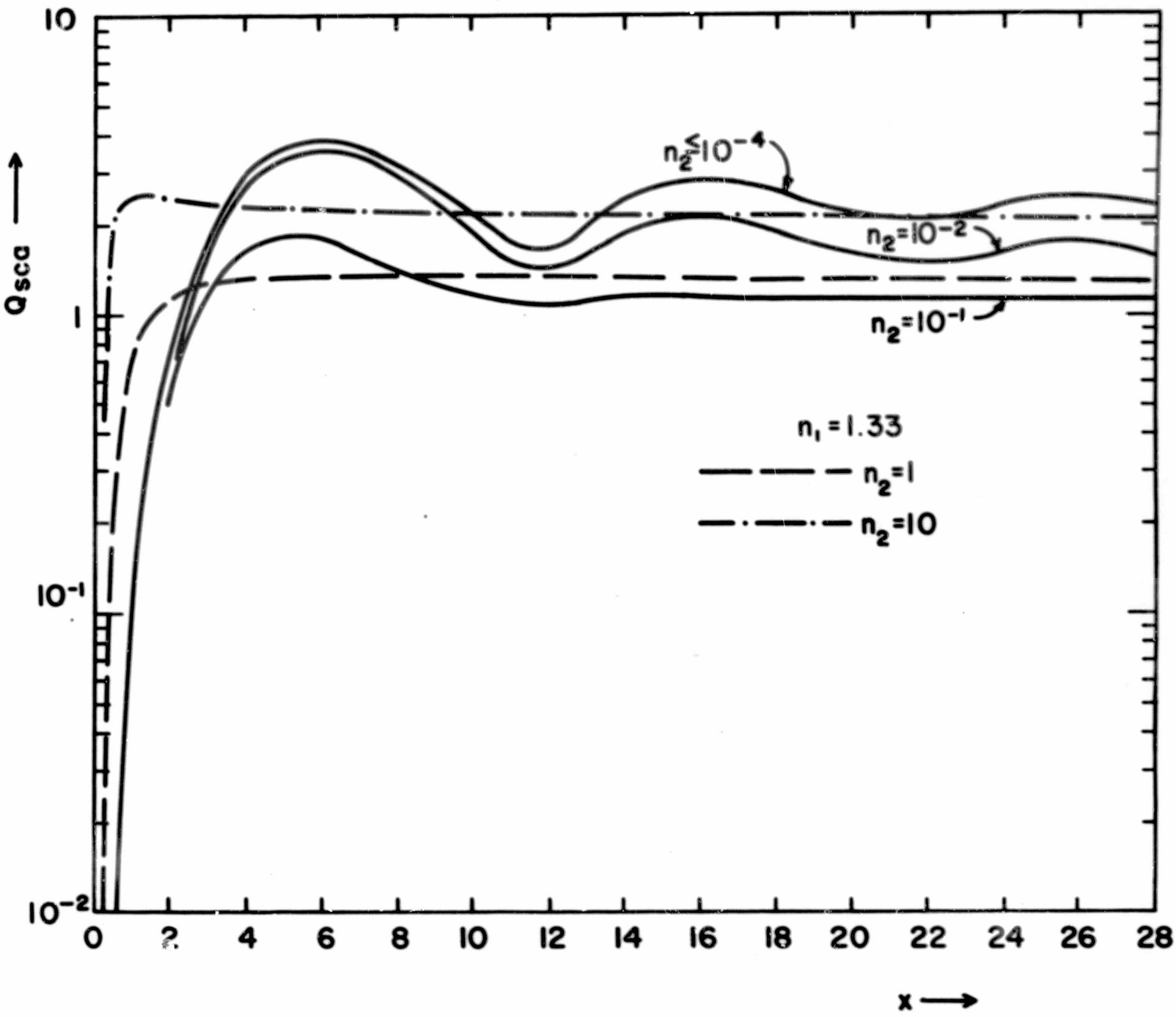
10
1
10^{-1}
10^{-2}
Q_{sca}
$n_2 \leq 10^{-4}$
$n_2 = 10^{-2}$
$n_2 = 10^{-1}$
$n_1 = 1.33$
$n_2 = 1$
$n_2 = 10$
0
2
4
6
8
10
12
14
16
18
20
22
24
26
28
x

FIGURE 6

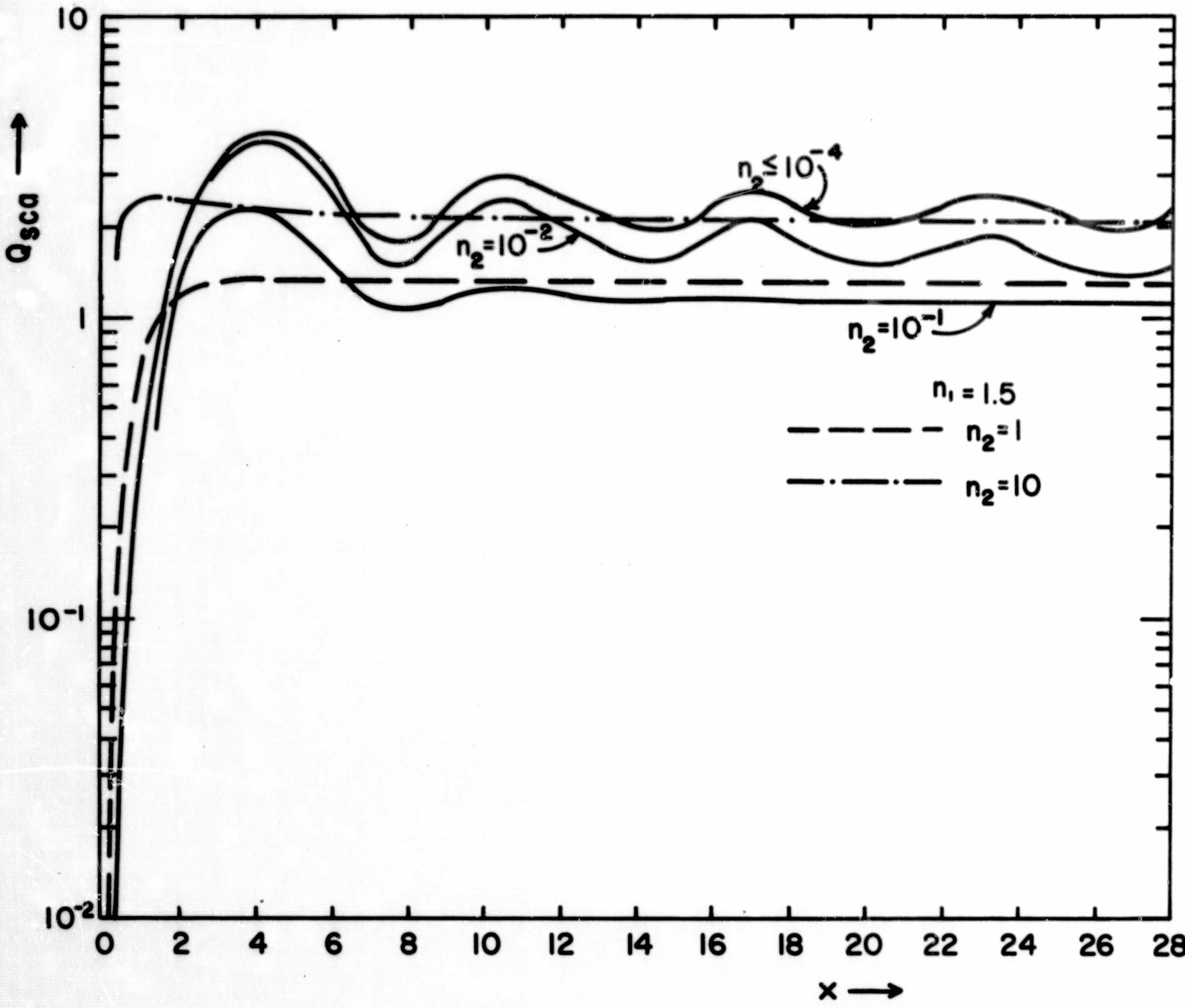
10
1
10^{-1}
10^{-2}
Q_{sca}
$n_2 \leq 10^{-4}$
$n_2 = 10^{-2}$
$n_2 = 10^{-1}$
$n_1 = 1.5$
$n_2 = 1$
$n_2 = 10$
0
2
4
6
8
10
12
14
16
18
20
22
24
26
28
x

FIGURE 7

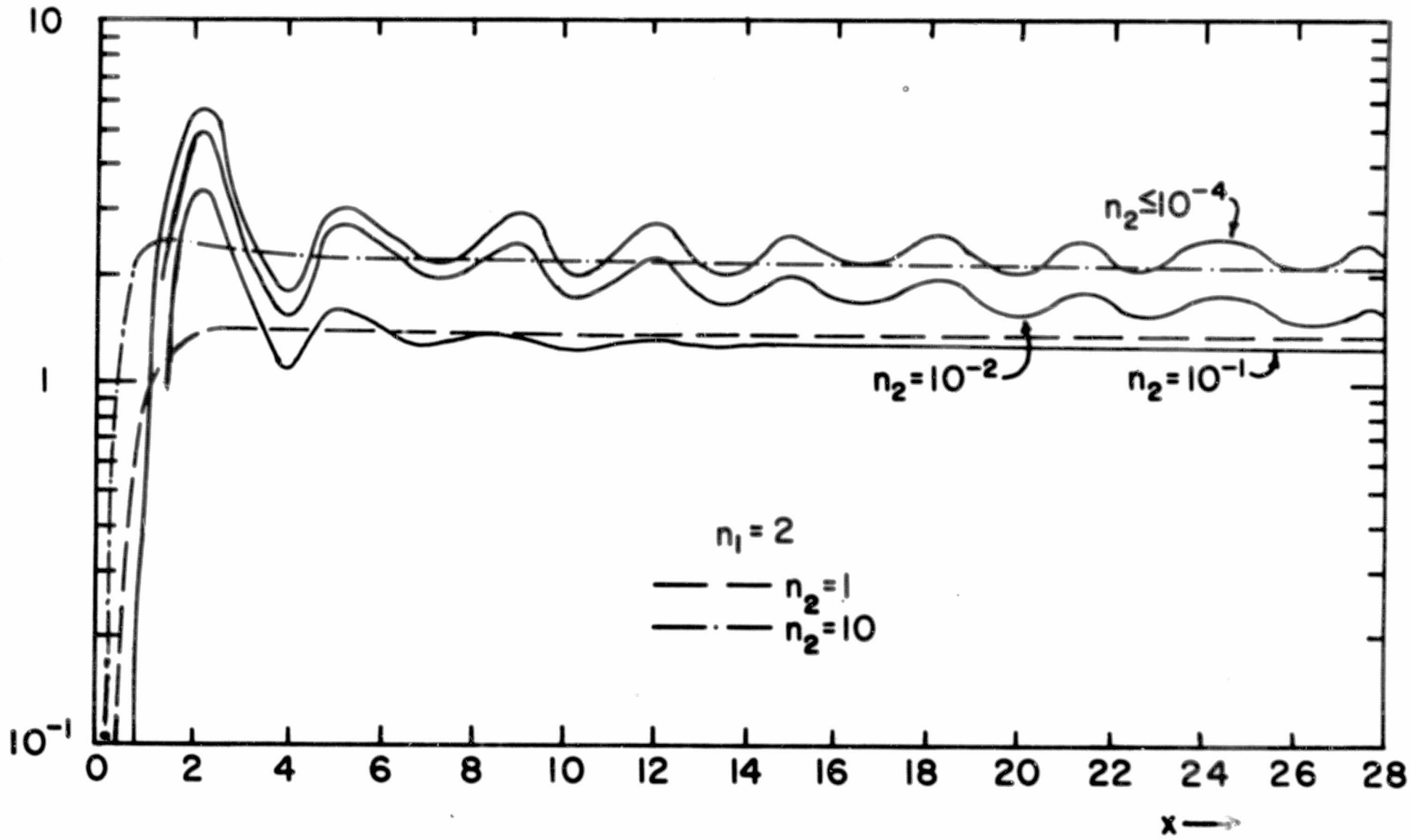
10
1
10^{-1}
Q_{sca} ⟶
$n_2 \leq 10^{-4}$
$n_2 = 10^{-2}$
$n_2 = 10^{-1}$
$n_1 = 2$
$n_2 = 1$
$n_2 = 10$
0 2 4 6 8 10 12 14 16 18 20 22 24 26 28
x ⟶

FIGURE 8

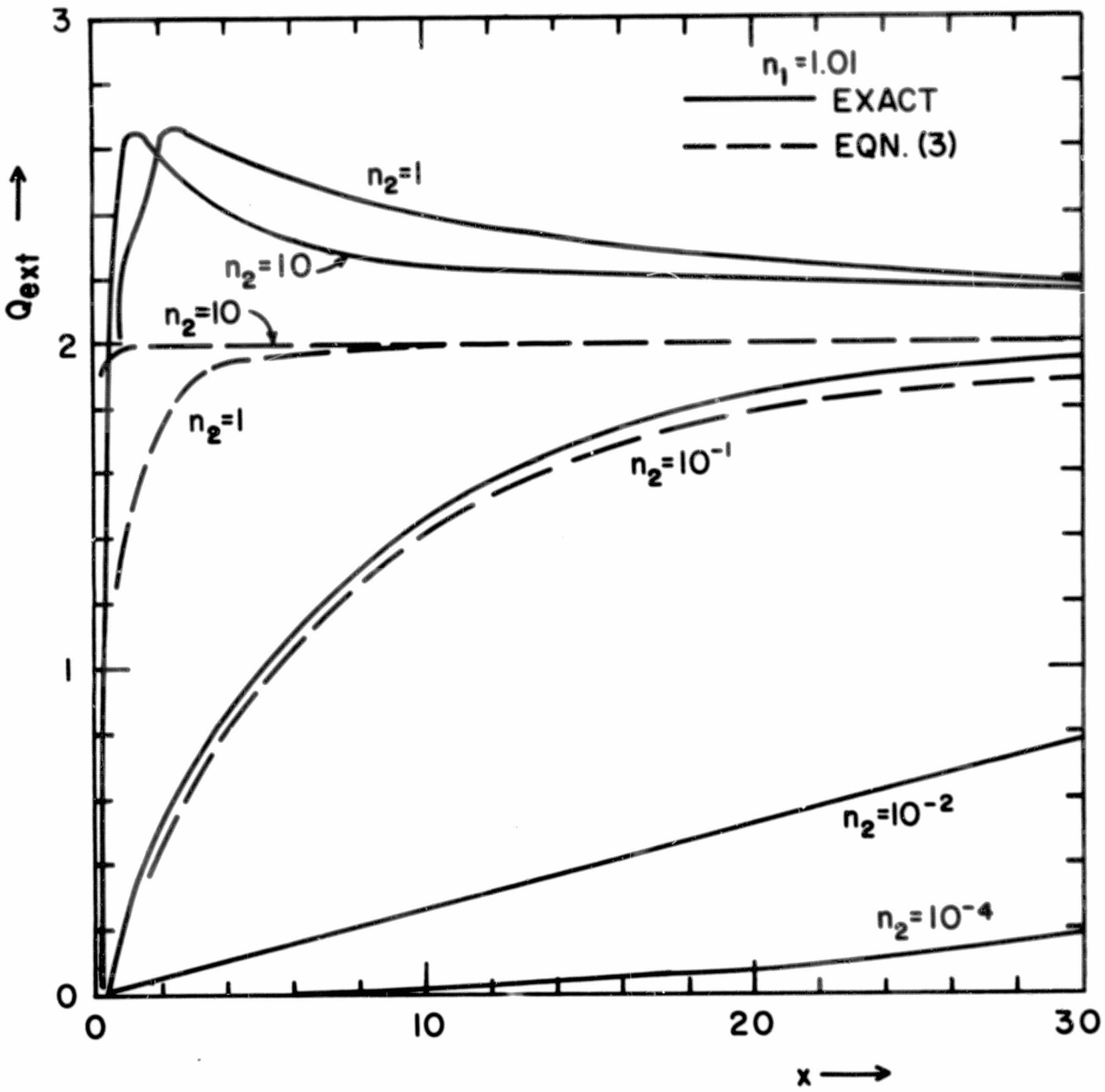
3
2
1
0
Q_{ext} ⟶
0
10
20
30
x ⟶
n_1=1.01
EXACT
EQN. (3)
n_2=1
n_2=10
n_2=10
n_2=1
n_2=10^{-1}
n_2=10^{-2}
n_2=10^{-4}

FIGURE 9

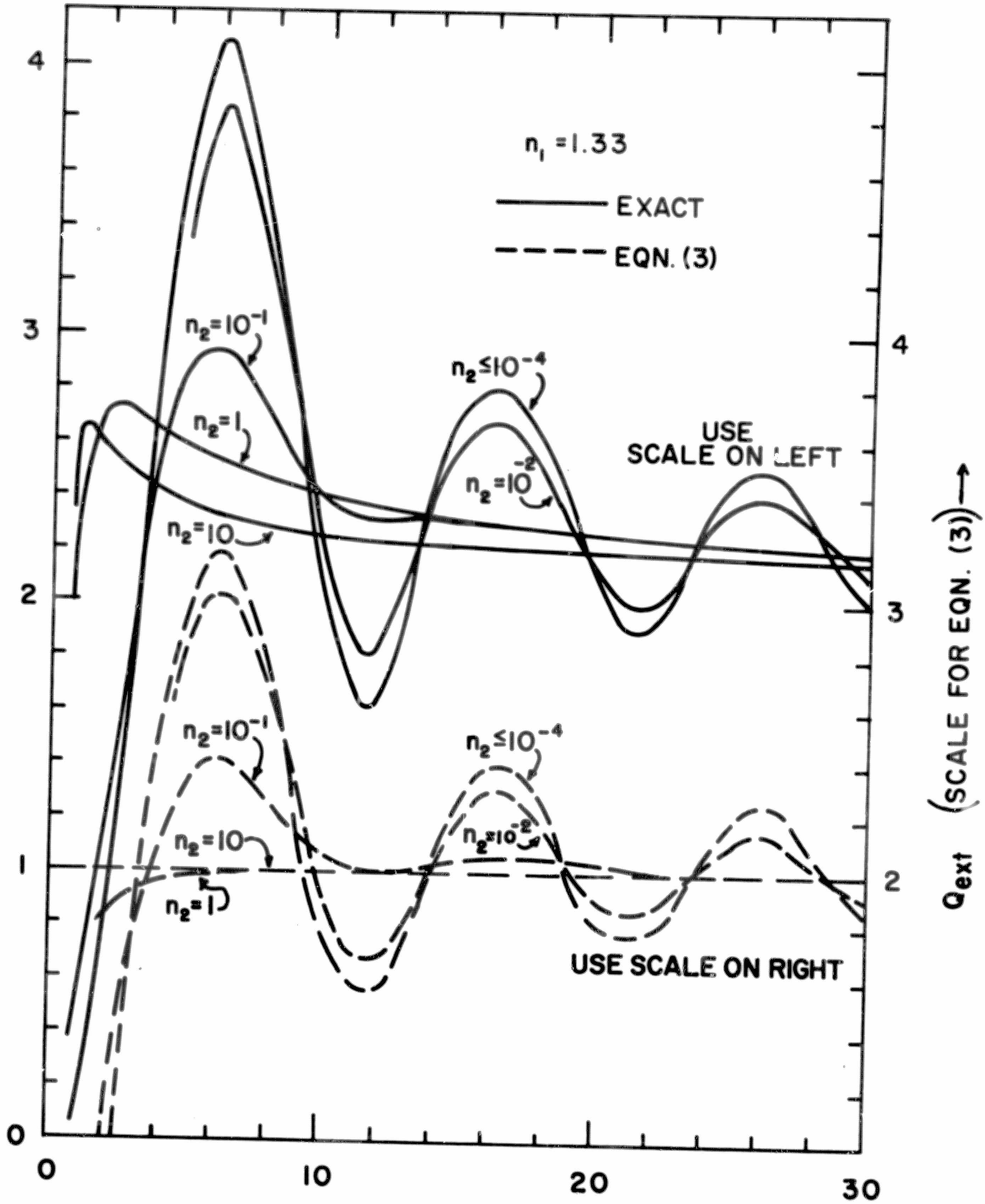
Q_{ext} (SCALE FOR EXACT EQUATION) ⟶
Q_{ext} (SCALE FOR EQN. (3)) ⟶
x ⟶
n_1 = 1.33
EXACT
EQN. (3)
n_2=10
n_2=1
n_2=10^{-1}
$n_2 \leq 10^{-4}$
n_2=10^{-2}
USE SCALE ON LEFT
USE SCALE ON RIGHT
0
1
2
3
4
0
10
20
30

FIGURE 10

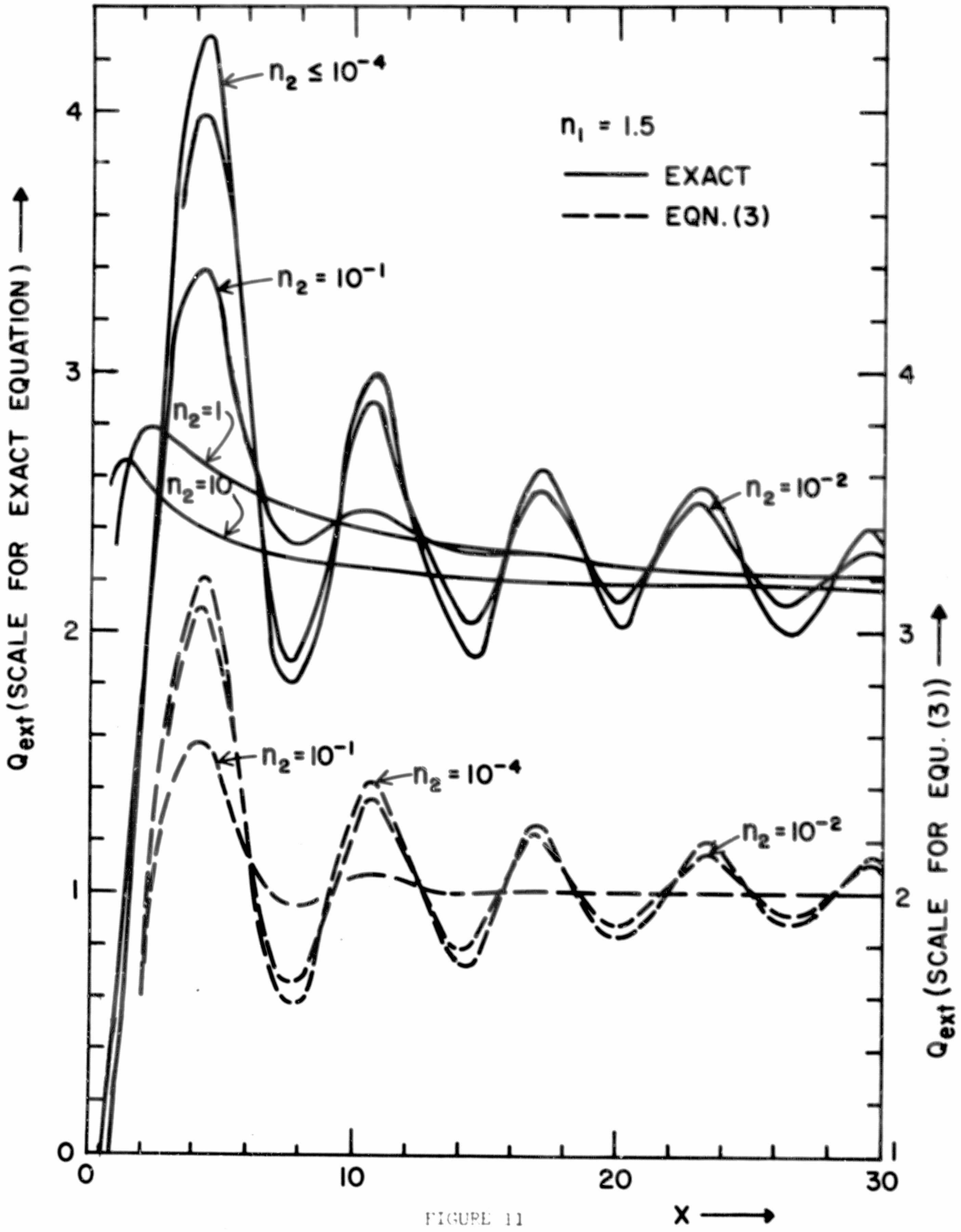
$n_2 \leq 10^{-4}$
$n_1 = 1.5$
EXACT
EQN. (3)
$n_2 = 10^{-1}$
$n_2 = 1$
$n_2 = 10$
$n_2 = 10^{-2}$
$n_2 = 10^{-1}$
$n_2 = 10^{-4}$
$n_2 = 10^{-2}$
Q_{ext} (SCALE FOR EXACT EQUATION) ⟶
Q_{ext} (SCALE FOR EQU. (3)) ⟶
X ⟶
0
1
2
3
4
10
20
30

FIGURE 11

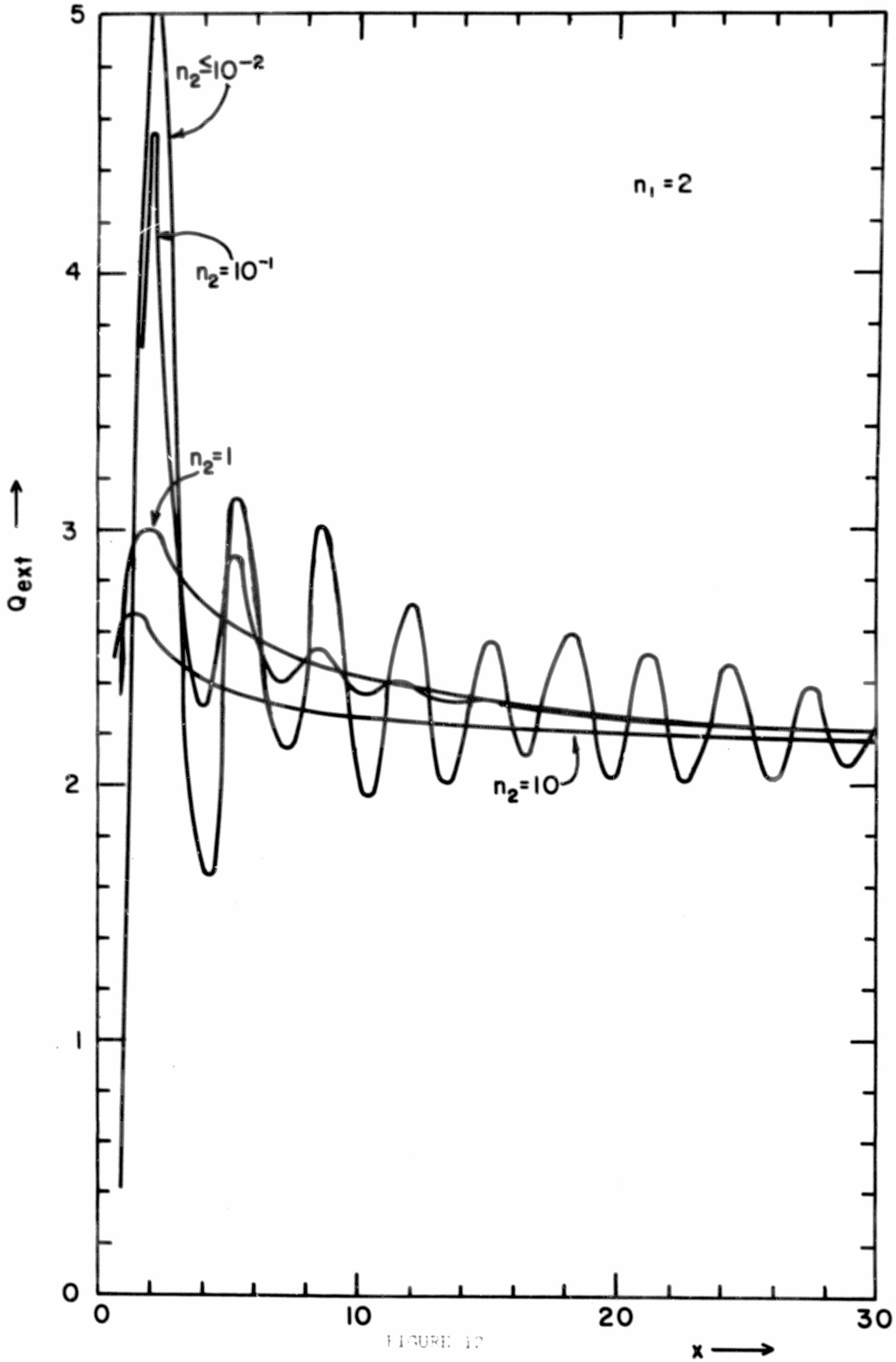

FIGURE 12

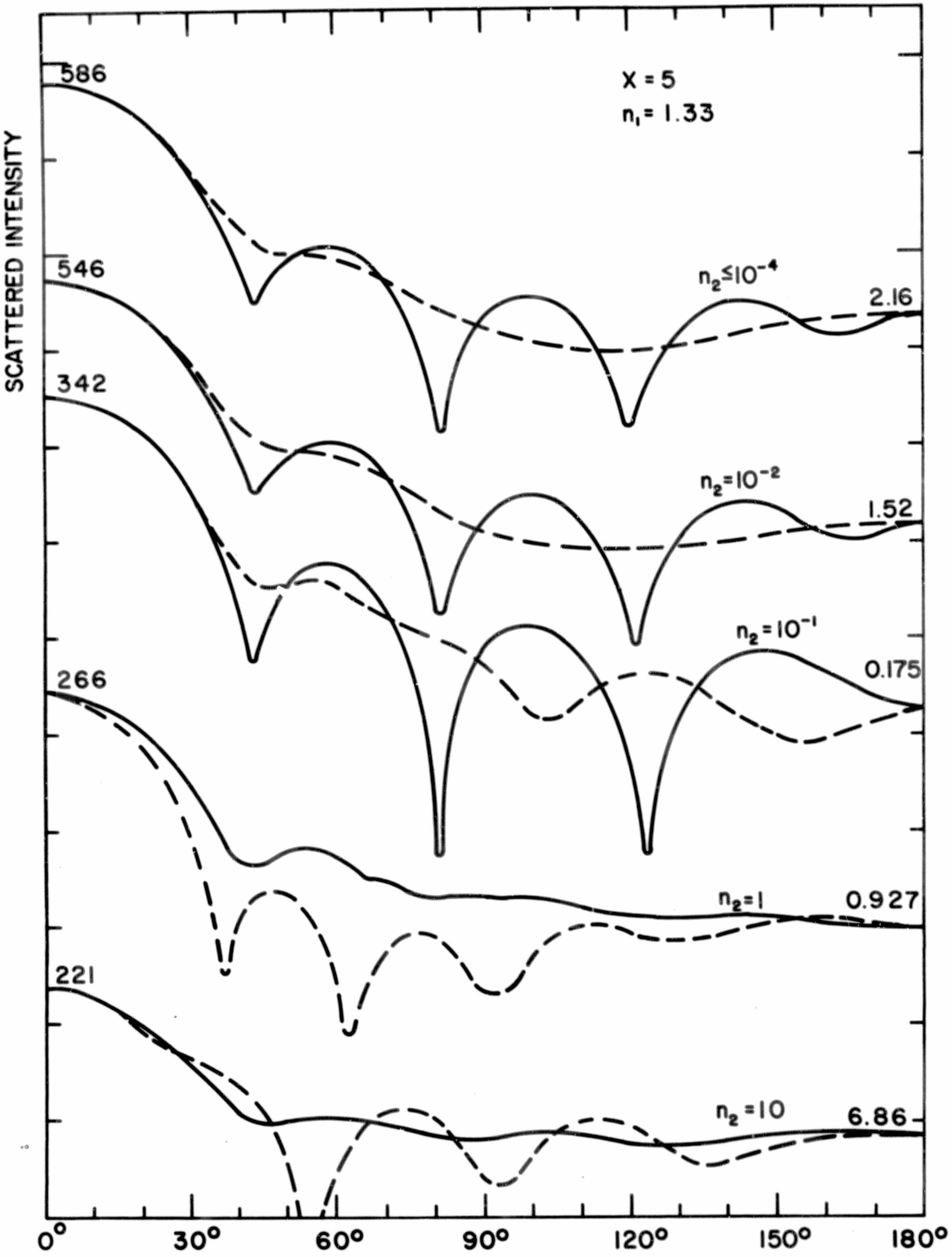
X = 5
n_1 = 1.33
586
546
342
266
221
$n_2 \leq 10^{-4}$
2.16
$n_2 = 10^{-2}$
1.52
$n_2 = 10^{-1}$
0.175
$n_2 = 1$
0.927
$n_2 = 10$
6.86
SCATTERED INTENSITY
0°
30°
60°
90°
120°
150°
180°
SCATTERING ANGLE

FIGURE 13

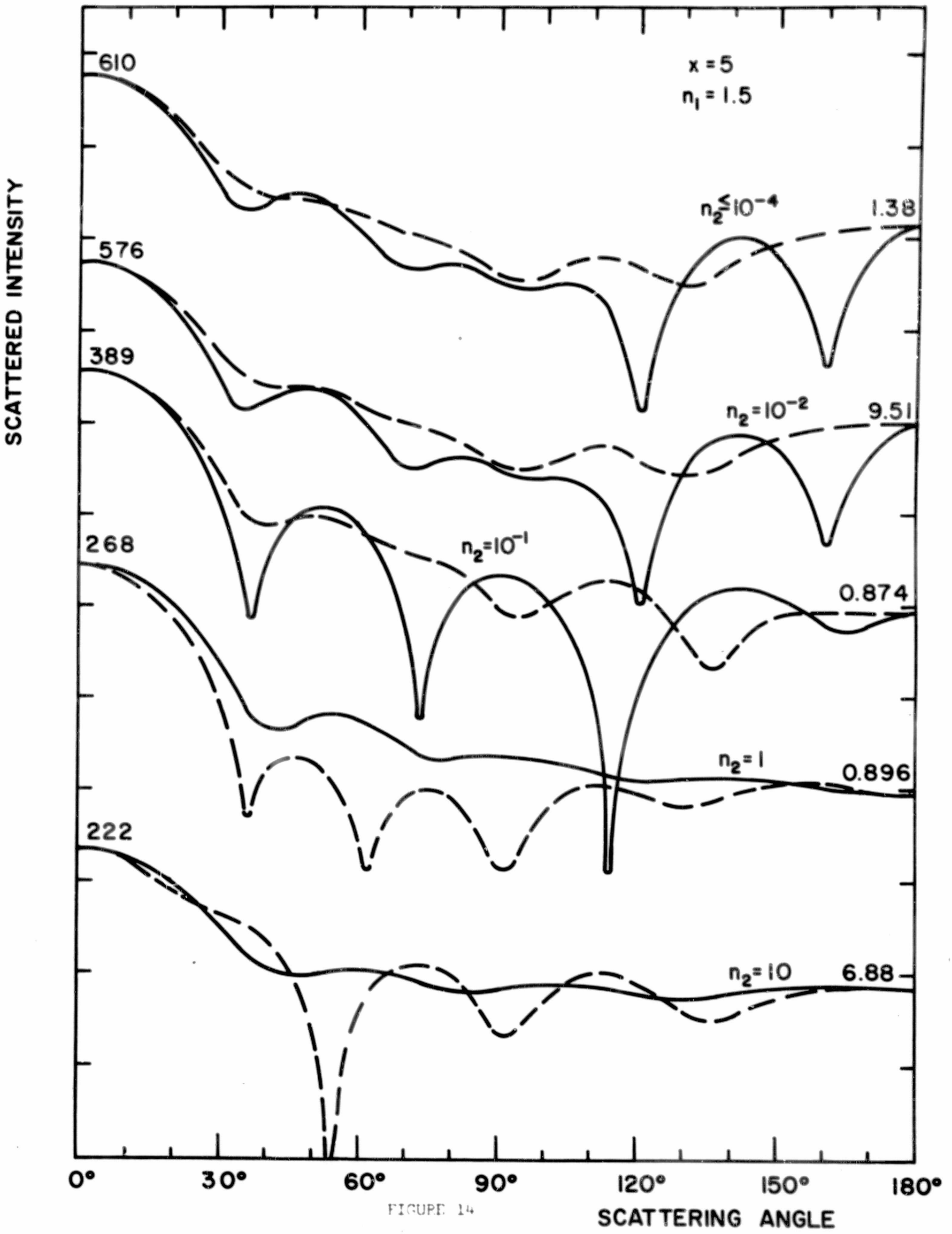
x = 5
n_1 = 1.5
610
576
389
268
222
$n_2 \leq 10^{-4}$
1.38
$n_2 = 10^{-2}$
9.51
$n_2 = 10^{-1}$
0.874
n_2 = 1
0.896
n_2 = 10
6.88
SCATTERED INTENSITY
0°
30°
60°
90°
120°
150°
180°
SCATTERING ANGLE

FIGURE 14

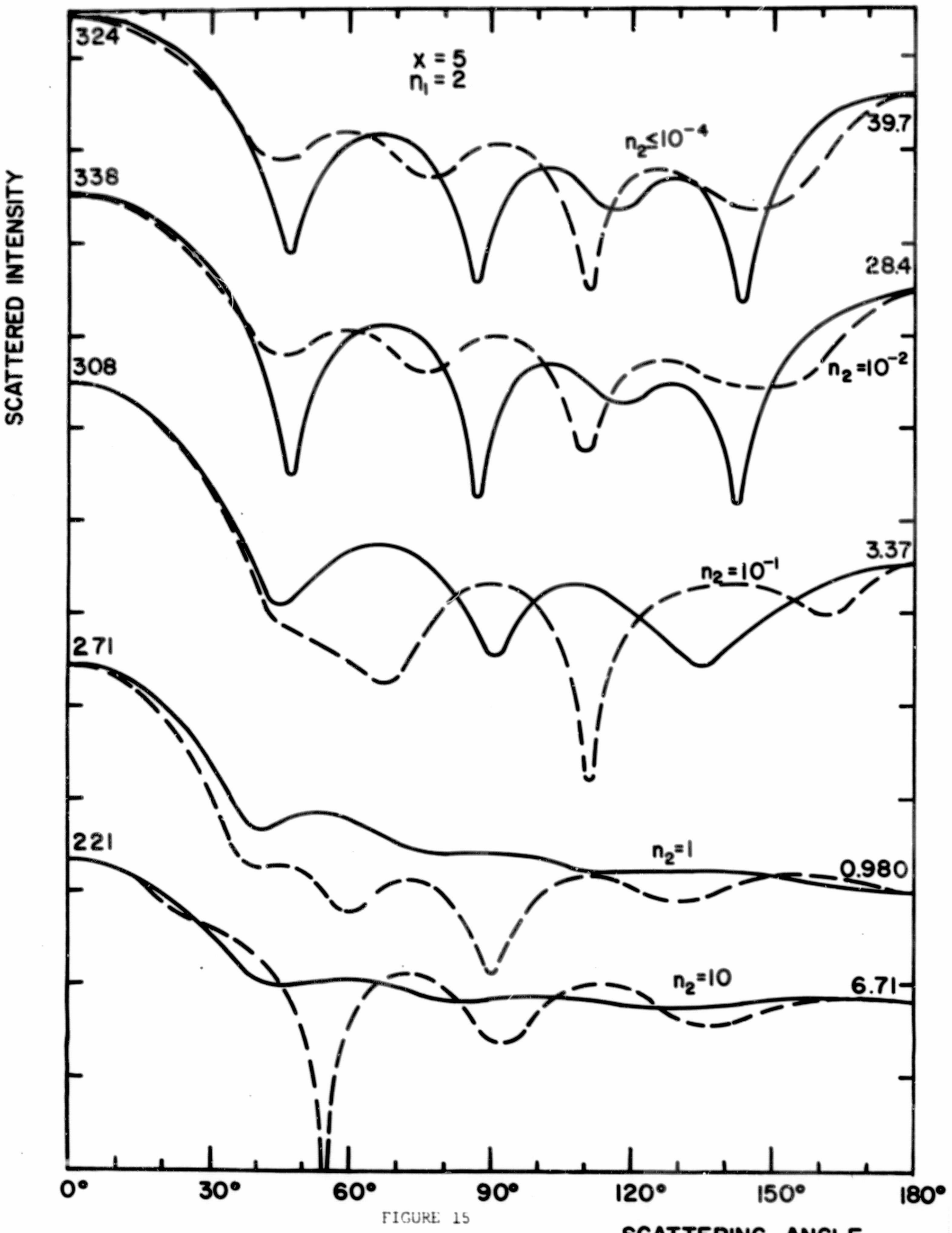
x = 5
n1 = 2
324
338
308
271
221
n2≤10⁻⁴
n2=10⁻²
n2=10⁻¹
n2=1
n2=10
39.7
28.4
3.37
0.980
6.71
SCATTERED INTENSITY
0°
30°
60°
90°
120°
150°
180°
SCATTERING ANGLE

FIGURE 15

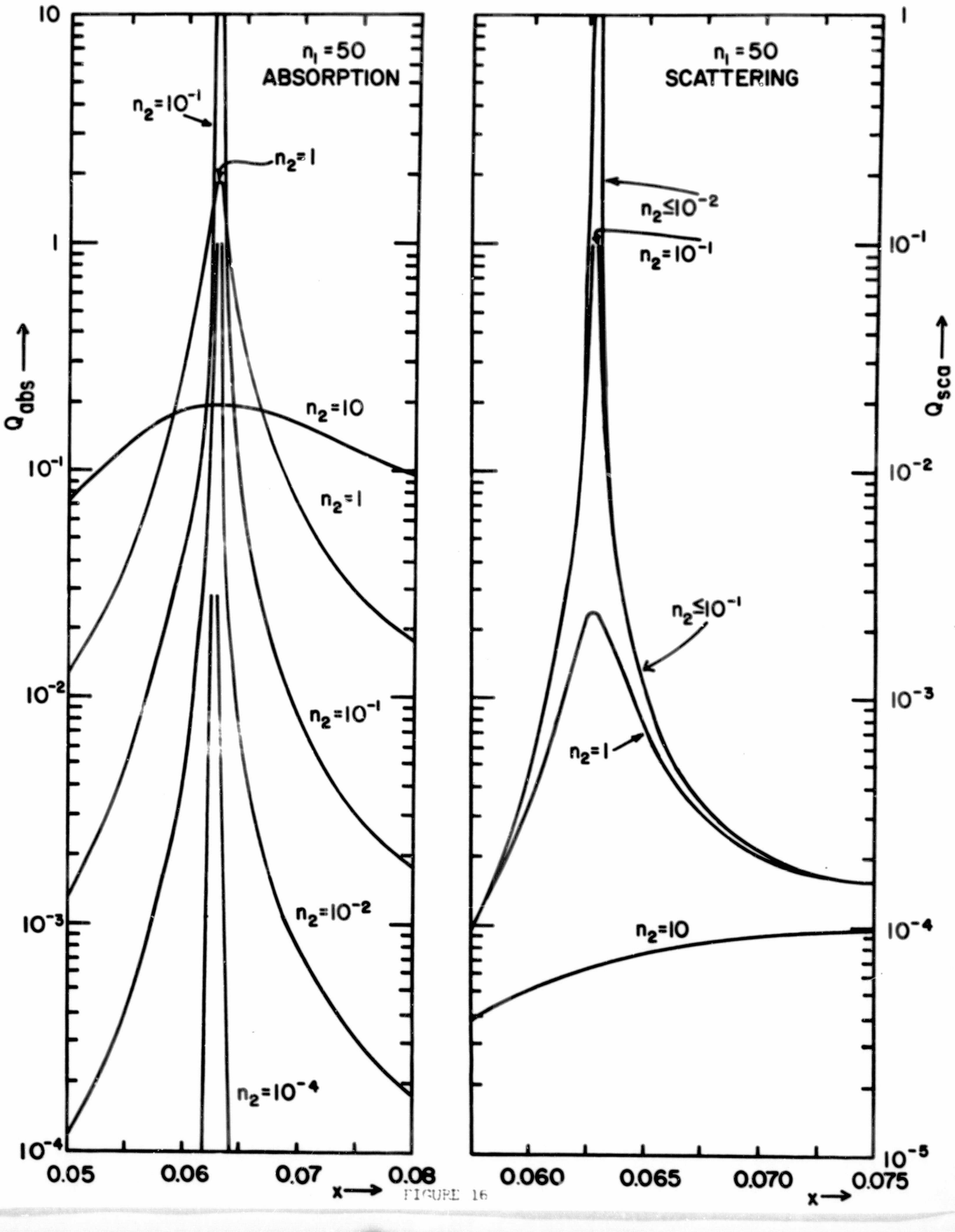
$n_1 = 50$
ABSORPTION
$n_2 = 10^{-1}$
$n_2 = 1$
$n_2 = 10$
$n_2 = 1$
$n_2 = 10^{-1}$
$n_2 = 10^{-2}$
$n_2 = 10^{-4}$
Q_{abs}
10
1
10^{-1}
10^{-2}
10^{-3}
10^{-4}
0.05
0.06
0.07
0.08
x
$n_1 = 50$
SCATTERING
$n_2 \leq 10^{-2}$
$n_2 = 10^{-1}$
$n_2 \leq 10^{-1}$
$n_2 = 1$
$n_2 = 10$
Q_{sca}
1
10^{-1}
10^{-2}
10^{-3}
10^{-4}
10^{-5}
0.060
0.065
0.070
0.075
x

FIGURE 16